Pramana – J. Phys. (2021) 95:197
https://doi.org/10.1007/s12043-021-02226-6

Large-amplitude dust inertial Alfvén waves in an electron-depleted dusty plasma

MANPREET SINGH[1,2], KULDEEP SINGH[2] and N S SAINI[2],*

[1]Department of Planetary Sciences-Lunar and Planetary Laboratory, University of Arizona, Tucson, AZ 85721, USA
[2]Department of Physics, Guru Nanak Dev University, Amritsar 143 005, India
*Corresponding author. E-mail: nssaini@yahoo.com

MS received 6 May 2021; revised 6 July 2021; accepted 13 July 2021

Abstract. The existence of the large-amplitude dust inertial Alfvén waves (DIAWs) has been presented in an electron-depleted, two-fluid dust-ion plasma. Linear analysis shows that the DIAWs travel slower than the dust Alfvén waves. DIAWs are the obliquely (with respect to the external magnetic field) propagating oscillations of dust density, having the characteristics of a solitary wave. In order to observe the nonlinear behaviour of the DIAWs, the Sagdeev pseudopotential method has been used to derive the energy balance equation and from the expression of the Sagdeev pseudopotential, the existence conditions for the DIAWs have also been determined. It is observed that density rarefactions travelling at sub- and super-Alfvénic speeds are associated with DIAWs.

Keywords. Dusty plasmas; inertial Alfvén waves; electron depleted; Sagdeev pseudopotential; solitary waves.

PACS Nos 52.35.Bj; 52.27.Lw; 52.35.Sb; 94.05.Fg; 52.35.–g

1. Introduction

Alfvén waves (AWs), since their prediction [1] and discovery [2], have played a vital role in understanding a vast majority of phenomena in space and astrophysical environments. AWs are the non-dispersive waves in which all the charged particles are frozen into the magnetic field. However, under suitable conditions, two types of dispersive AWs, namely kinetic Alfvén waves (KAWs) and inertial Alfvén waves (IAWs) are formed. When the plasma β is in the range: $m_e/m_i \ll \beta \ll 1$ [where $m_e(m_i)$ is the electron(ion) mass and plasma-$\beta = (8\pi n_{i0} k_B T_i)/B_0^2$, n_{i0} is the ion number density at equilibrium, k_B is the Boltzmann constant, T_i is the ion temperature], the KAWs are formed. In this case, the electron thermal velocity $v_{te} = (k_B T_e/m_e)^{1/2}$ (where T_e is the electron temperature) becomes greater than the Alfvén velocity $V_A (= B_0/(4\pi n_{i0} m_i)^{1/2})$ and the parallel electron pressure causes the wave dispersion. On the other hand, when $\beta \ll m_e/m_i \ll 1$, the IAWs are formed. For IAWs, the electron thermal velocity (v_{te}) remains less than the Alfvén velocity (V_A), and the electron inertia plays a significant role in the wave dispersion. In the case of dispersive Alfvén waves, the charge separation occurs when the perpendicular wave number is very large compared to the parallel wave number. Since the electron gyroradius is small compared to ion gyroradius, the electrons keep on following the magnetic lines of force, while the ions respond to the large perpendicular wave number. Both KAWs and IAWs are quasi-electrostatic waves in which electromagnetic mode is coupled to the electrostatic ion-acoustic mode [3]. IAWs have parallel electric field which is generated due to the electron inertia [4]. IAWs play significant roles in auroral electron acceleration [5].

The observations from the Cassini and Voyager space missions have confirmed an abundance of dust particulates in Saturnian spokes [6]. Numerous investigations have reported that such kind of dust grains are omnipresent in various space environments (e.g., solar nebulae, comet tails etc.) [6,7] as well as in laboratory (e.g., manufacturing and processing of semiconductor devices, etc.) [8,9]. Presence of heavy micron-sized charged dust particles in the electron–ion plasma modifies the linear and nonlinear behaviour of the plasma waves. Over the past three decades, numerous researchers have examined the different dust-acoustic nonlinear coherent structures (i.e., solitons, shocks, double layers, rogons, etc.) in magnetised/unmagnetised space dusty plasmas in the framework of reductive

Published online: 18 November 2021

perturbation approach and Sagdeev pseudopotential method [10–19]. Due to the large size of the dust grains, electrons can stick to the dust grain surface. This leads to a significant depletion of electron density. However, complete depletion of electron density is not possible in such a plasma [20]. In this situation, the charge on the dust grains can reach up to several thousands of electronic charge. This electron-depleted plasma can support a variety of electrostatic and electromagnetic solitary waves. For the existence of dust-acoustic solitary waves in an electron-depleted dusty plasma, the ions provide the restoring force while the dust mass provides the necessary inertia. As the electron population as well as mass are very small compared to that of ions and dust grains, the electrons do not contribute towards wave formation. In the presence of a magnetic field, the dust fluid can respond to the perturbations in the magnetic field. Thus, the polarisation drift of the dust gives rise to the dust kinetic Alfvén solitary waves (DKASWs). These waves occur when the perpendicular wavelength is comparable to dust-acoustic gyroradius and the dust plasma β, β_d ($= 4\pi n_{d0} k_B T_i / B_0^2$, where n_{d0} is the dust number density at equilibrium) is in the range $m_i/m_d \ll \beta_d \ll 1$ [21]. In the case of DKASWs the ion thermal speed is higher than the dust Alfvén speed. The parallel electric field is caused by the parallel ion current. DKASWs in electron-depleted dust-ion plasma were studied by Mirza *et al* [22]. They observed sub-Alfvénic compressive and rarefactive DKASWs and super-Alfvénic compressive DKASWs. The characteristics of DKASWs were significantly modified by the Mach number and angle of propagation with respect to the magnetic field. The coupled dust-acoustic waves (DAWs) and DKASWs were studied by Mahmood and Saleem [23] in a dust-ion and dust-ion-electron plasmas. The characteristics of these modes were significantly modified by the plasma β. Saini *et al* [24] illustrated the small-amplitude DKASWs and dust kinetic Alfvén rogue waves (DKARWs) in an electron-depleted dusty plasma containing two temperature q-non-extensive distributed ions. It was observed that the plasma β, angle of propagation, non-extensivity of ions and concentration of ions have significant influence on the characteristics of both DKASWs as well as DKARWs. In the past two decades, DKASWs have also been studied by several researchers in different dusty plasma systems by taking a non-zero electron density [25–27].

In a magnetised electron-depleted dust-ion plasma, when the ion thermal speed becomes lower than the dust-Alfvén speed, the ion inertia can play a significant role in wave dispersion. In this case, the parallel electric field is generated by the slow moving ions in the parallel direction. Thus, the ions can have fluid-like characteristics in the parallel direction. In this situation, when β_d is in the range $\beta_d \ll m_i/m_d \ll 1$, a slow moving wave can be formed which is named as the dust inertial Alfvén wave (DIAW). DIAWs are formed when the perpendicular wavelength is comparable to effective inertial length λ_{eff} (i.e., $k_\perp \lambda_{\text{eff}} \approx 1$), where $k_\perp$ is the perpendicular wave vector of the wave,

$$\lambda_{\text{eff}} = \frac{c}{(\omega_{pi}^2 + \omega_{pd}^2)^{1/2}}.$$

c is the speed of light and $\omega_{pi}(\omega_{pd})$ is the ion(dust) plasma frequency. The DIAWs have speed less than the dust-Alfvén speed. The existence of DIAWs has not been reported in literature so far. This motivates us to study the characteristics of DIAWs in an electron-depleted two-fluids dust- and ion-plasma. The manuscript is organised as follows: The model equations governing the dynamics of the dust and ion fluids are described in §2. The linear analysis is presented in §3. The nonlinear analysis is carried out to derive the energy balance equation by using the Sagdeev pseudopotential method in §4. The conditions for the existence of solitary DIAWs are illustrated in §5. The parametric analysis is presented in §6. The overall conclusions are highlighted in §7.

2. Fluid model equations

We consider a magnetised electron-depleted dusty plasma, comprising negatively charged dust fluid (number density n_d and mass m_d) and positively charged ions (number density n_i and mass m_i). Electrons are considered to be significantly depleted because of their attachment to the dust grain surface. The background magnetic field B_0 is directed along the positive z-axis. The dust plasma beta (β_d) is considered to be low, such that $\beta_d \ll m_i/m_d$. The low β assumption gives rise to two distinct electric potentials $\phi_\perp$ (perpendicular to B_0) and $\psi_\parallel$ (parallel to B_0) with respective electric fields $E_x = -\partial\phi_\perp/\partial x$ and $E_z = -\partial\psi_\parallel/\partial z$ [28]. The wave is considered to be travelling in the x–z plane. In the presence of a strong magnetic field, the ions get strongly magnetised in the direction of the magnetic field. Under this condition, ions can freeze into the magnetic field and act as a fluid in the direction of the magnetic field. On the other hand, when the perpendicular wavelength is comparable to the ion inertial length, charge separation occurs and the dust particles no longer follow the magnetic lines of force. As a result of this charge separation, the dust Alfvén waves can couple to the electrostatic modes to excite the so-called dust inertial Alfvén waves. Thus, ions and dust particles can behave as two different fluids because of the large differences in their masses and gyroradii. The dynamics of the ions and dust fluids

are described by the fluid model equations [29,30] in the following form.

The ion continuity and momentum equations are expressed respectively as

$$\frac{\partial n_i}{\partial t} + \nabla \cdot (n_i \mathbf{v_i}) = \mathbf{0} \tag{1}$$

and

$$\frac{\partial \mathbf{v_i}}{\partial t} + (\mathbf{v_i} \cdot \nabla)\mathbf{v_i} = \frac{Z_i e}{m_i}\left(E + \frac{\mathbf{v_i} \times \mathbf{B}}{c}\right), \tag{2}$$

where $\mathbf{v_i}$ is the ion fluid velocity and $\mathbf{E}$ is the electric field. Similarly, the continuity and momentum equations for the dust fluid are given respectively as

$$\frac{\partial n_d}{\partial t} + \nabla \cdot (n_d \mathbf{v_d}) = \mathbf{0} \tag{3}$$

and

$$\frac{\partial \mathbf{v_d}}{\partial t} + (\mathbf{v_d} \cdot \nabla)\mathbf{v_d} = -\frac{Z_d e}{m_d}\left(E + \frac{\mathbf{v_d} \times \mathbf{B}}{c}\right), \tag{4}$$

where $\mathbf{v_d}$ is the dust fluid velocity. The Faraday and Ampere's laws yield respectively

$$\nabla \times \mathbf{E} = -\frac{1}{c}\frac{\partial \mathbf{B}}{\partial t} \quad \text{and} \quad \nabla \times \mathbf{B} = \frac{4\pi}{c}\mathbf{J}, \tag{5}$$

where $\mathbf{J} = J_z \hat{z}$ is the parallel ion current density. The variation in all the variables are assumed to be in the x–z plane which results in $(\partial/\partial y) = 0$. However, the magnetic field has an induced component in the y-direction. In a low β plasma, two-potential theory is applicable [28] having parallel ($\psi_\parallel$) and perpendicular ($\phi_\perp$) potentials with their respective electric fields

$$E_x = -\frac{\partial \phi_\perp}{\partial x}, \quad E_y = 0 \quad \text{and} \quad E_z = -\frac{\partial \psi_\parallel}{\partial z}. \tag{6}$$

Expanding eqs (5), one obtains

$$\frac{\partial^2(\phi_\perp - \psi_\parallel)}{\partial x \partial z} = \frac{1}{c}\frac{\partial B_y}{\partial t} \tag{7}$$

and

$$\frac{\partial^2 B_y}{\partial x \partial z} = \frac{4\pi}{c}\frac{\partial J_z}{\partial z}. \tag{8}$$

The current continuity equation is given as

$$\frac{\partial J_z}{\partial z} = -e\left[Z_i \frac{\partial n_i}{\partial t} + Z_d \frac{\partial (n_d v_{dz})}{\partial z}\right]. \tag{9}$$

Thus, writing eqs (1)–(4) in the component form and combining eqs (7)–(9), the set of fluid equations are obtained in the following form:

$$\frac{\partial n_i}{\partial t} + \frac{\partial (n_i v_{iz})}{\partial z} = 0, \tag{10}$$

$$\frac{\partial v_{iz}}{\partial t} + v_{iz}\frac{\partial v_{iz}}{\partial z} = -\frac{Z_i e}{m_i}\frac{\partial \psi_\parallel}{\partial z}, \tag{11}$$

$$\frac{\partial n_d}{\partial t} + \frac{\partial (n_d v_{dx})}{\partial x} + \frac{\partial (n_d v_{dz})}{\partial z} = 0. \tag{12}$$

In the low-frequency limit, $|\partial_t| \ll \Omega_d$ for dust polarisation drift and the dust equation of motion can be described as

$$v_{dx} = \frac{c}{B_0 \Omega_d}\frac{\partial^2 \phi_\perp}{\partial x \partial t}, \tag{13}$$

$$\frac{\partial v_{dz}}{\partial t} + v_{dx}\frac{\partial v_{dz}}{\partial x} + v_{dz}\frac{\partial v_{dz}}{\partial z} = \frac{Z_d e}{m_d}\frac{\partial \psi_\parallel}{\partial z}, \tag{14}$$

where v_{iz} is the parallel fluid velocity of the ions, v_{dx} and v_{dz} are the transverse and parallel fluid velocities of dust respectively, e is the elementary charge, $Z_i(Z_d)$ is the ion(dust) charge number, c is the velocity of light and $\Omega_d = Z_d e B_0/m_d c$ is the dust cyclotron frequency. For the dust motion perpendicular to the magnetic field B_0, the convective derivative term $(\mathbf{v_d} \cdot \nabla)\mathbf{v_d}$ can be neglected [31,32] and this leads to eq. (13).

The Faraday and Ampere's laws in the simplified forms can be written respectively as

$$\frac{\partial^2(\phi_\perp - \psi_\parallel)}{\partial x \partial z} = \frac{1}{c}\frac{\partial B_y}{\partial t} \tag{15}$$

and

$$\frac{\partial^2 B_y}{\partial x \partial z} = -\frac{4\pi e}{c}\left[Z_i \frac{\partial n_i}{\partial t} + Z_d \frac{\partial (n_d v_{dz})}{\partial z}\right]. \tag{16}$$

The quasi-neutrality condition is given as

$$Z_d n_d = Z_i n_i. \tag{17}$$

3. Linear analysis

In this section, we have derived a linear dispersion relation of DIAWs. Linearising eqs (10)–(17) and assuming all the perturbed quantities to be of the form $e^{i(k_\perp x + k_\parallel z - \omega t)}$ (where $k_\perp(k_\parallel)$ is the perpendicular(parallel) component of the wave vector and ω is the frequency of oscillations), the following dispersion relation is obtained:

$$\omega = \frac{V_{Ad} k_\parallel}{\sqrt{1 + k_\perp^2 \lambda_{\text{eff}}^2}}, \tag{18}$$

where

$$\lambda_{\text{eff}} = \frac{c}{\sqrt{\omega_{pi}^2 + \omega_{pd}^2}}$$

is the effective inertial length and

$$V_{Ad} = B_0/(4\pi n_{d0} m_d)^{1/2}$$

is the dust Alfvén speed. Here,

$$\omega_{pd} = (4\pi n_{d0} Z_d^2 e^2/m_d)^{1/2}$$

and

$$\omega_{pi} = (4\pi n_{i0} Z_i^2 e^2/m_i)^{1/2}$$

are the dust and ion plasma frequencies respectively. It is interesting to observe that the dispersion relation is modified by the ion and dust plasma frequencies. The term λ_{eff} has the dimensions of length and can be considered as the effective inertial length. Thus, when the perpendicular wavelength is comparable to λ_{eff}, i.e., $k_\perp \lambda_{\text{eff}} \approx 1$, dispersion of the wave occurs. It can be seen that the dispersion relation is independent of the temperature of either species. However, it is a function of masses m_d and m_i. This indicates that the inertia of particles are responsible for the dispersion of the wave. In the limiting case, when $k_\perp^2 \lambda_{\text{eff}}^2 < 1$, the above dispersion relation of DIAWs (given by eq. (18)) reduces to the well-known dispersion relation of dust Alfvén waves (i.e., $\omega = k_\parallel V_{Ad}$).

It is seen from eq. (18) that the ion inertial length has modified the dispersion relation. In the linear regime, DIAWs can be formed when the perpendicular wavelength develops to the scale of ion inertial length. In DIAWs, parallel electric field is caused by the ion inertia and the ion thermal speed is much lower than the dust Alfvén speed. In this case

$$\beta_d \frac{m_d}{m_i} = \frac{v_{thi}^2}{V_{Ad}^2} < 1. \tag{19}$$

Thus, it is realised that the DIAWs can propagate only when $\beta_d < (m_i/m_d) < 1$. In order to get more insight into the topology of the dispersion curves, we have considered a fixed value of θ in such a way that $k_\perp \gg k_\parallel$ (i.e., $\theta \lesssim \pi/2$, $k_\parallel = k\cos\theta$ and $k_\perp = k\sin\theta$) and plotted figure 1 for the variation of frequency (ω) of the DIAWs. It is seen that the phase velocity of DIAWs is very small compared to the phase velocity of the dust Alfvén waves. The dust Alfvén waves are non-dispersive electromagnetic waves while the DIAWs are dispersive quasi-electrostatic waves. It is noticed that the phase velocity of dust Alfvén waves is $(1 + k_\perp^2 \lambda_{\text{eff}}^2)^{1/2}$ times larger than that of the DIAWs. Moreover, the group velocity of the DIAWs is negative which means that waves propagate in backward direction. Thus, it confirms that the DIAWs are slow-moving waves having negative perpendicular group velocity.

4. Nonlinear analysis

The balance between dispersion and nonlinearity leads to the formation of solitary DIAWs. Before performing the nonlinear analysis, we normalise the different quantities in eqs (10)–(17) with the following scaling parameters: number density $N_j = n_j/n_{j0}$ (where

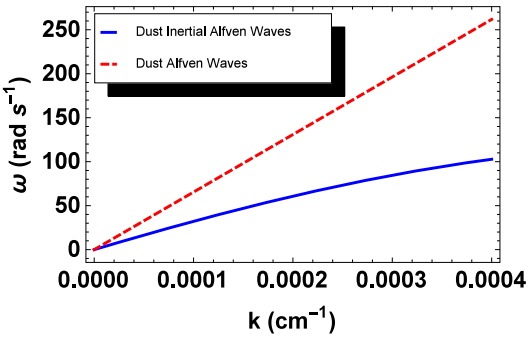

Figure 1. The frequency (ω) of DIAWs vs. k for fixed values of $B_0 = 3 \times 10^4$ G, $Z_i = 1$, $Z_d = 10^4$, $n_{i0} = 10^8$ cm^{-3}, $n_{d0} = 10^6$ cm^{-3} and $k_B T_i = 2$ eV.

$j = i, d$ and n_{j0} denotes the number density at equilibrium), potentials $(\phi, \psi) = e(\phi_\perp, \psi_\parallel)/k_B T_i$, velocity $V_l = v_l/V_{Ad}$ (where $l = iz, dx, dz$), time $T = t\Omega_d$ and space coordinates $(X, Z) = \omega_{pd}(x, z)/c$. Thus, the set of fluid equations in the normalised form are expressed as

$$\frac{\partial N_i}{\partial T} + \frac{\partial (N_i V_{iz})}{\partial Z} = 0, \tag{20}$$

$$\frac{\partial V_{iz}}{\partial T} + V_{iz}\frac{\partial V_{iz}}{\partial Z} = -\frac{\beta_d}{2\nu_m}\frac{\partial \psi}{\partial Z}, \tag{21}$$

$$\frac{\partial N_d}{\partial T} + \frac{\partial (N_d V_{dx})}{\partial X} + \frac{\partial (N_d V_{dz})}{\partial Z} = 0, \tag{22}$$

$$V_{dx} = \frac{\beta_d}{2}\frac{\partial^2 \phi}{\partial X \partial T}, \tag{23}$$

$$\frac{\partial V_{dz}}{\partial T} + V_{dx}\frac{\partial V_{dz}}{\partial X} + V_{dz}\frac{\partial V_{dz}}{\partial Z} = \frac{\beta_d}{2}\frac{\partial \psi}{\partial Z}, \tag{24}$$

$$\frac{\partial^4 (\phi - \psi)}{\partial X^2 \partial Z^2} = -\frac{2}{\beta_d}\left[\frac{\partial^2 N_i}{\partial T^2} + \frac{\partial^2 (N_d V_{dz})}{\partial T \partial Z}\right] \tag{25}$$

and

$$N_i = N_d, \tag{26}$$

where $\nu_m = Z_d m_i / Z_i m_d$ and eq. (25) is obtained by combining eqs (15) and (16).

Nonlinear DIA solitary waves can be studied by using the Sagdeev pseudopotential method, by transferring eqs (20)–(25) to the new moving coordinate system: $\xi = K_x X + K_z Z - M_{Ad} T$ (where $K_x(K_z)$ is the direction cosine in the $x(z)$-direction such that $K_x^2 + K_z^2 = 1$). $M_{Ad} = V/V_{Ad}$ is the dust Alfvén Mach number analogous to sound Mach number and V represents the speed of the nonlinear structures. The use of new moving coordinate system in eqs (20) and (21) respectively yields

$$-M_{Ad}\frac{\partial N_i}{\partial \xi} + K_z \frac{\partial (N_i V_{iz})}{\partial \xi} = 0 \tag{27}$$

and

$$-M_{Ad}\frac{\partial V_{iz}}{\partial \xi}+\frac{K_z}{2}\frac{\partial (V_{iz}^2)}{\partial \xi}=-\frac{\beta_d K_z}{2\nu_m}\frac{\partial \psi}{\partial \xi}. \tag{28}$$

The integration of the above equations under the boundary conditions, $\xi \to \pm\infty$, $N_i = 1$ and $V_{iz} = 0$, leads to

$$V_{iz}=\frac{M_{Ad}}{K_z}\left(1-\frac{1}{N_i}\right) \tag{29}$$

and

$$\frac{\mathrm{d}\psi}{\mathrm{d}\xi}=2\frac{\nu_m}{\beta_d}\frac{M_{Ad}^2}{K_z^2}\frac{1}{N_i^3}\frac{\mathrm{d}N_i}{\mathrm{d}\xi} \tag{30}$$

respectively. Similarly, from eqs (22)–(24), by using the boundary conditions, $\xi \to \pm\infty$, $N_d = 1$ and $V_{dx} = V_{dz} = 0$, we respectively obtain

$$V_{dx}=\frac{1}{K_x}\left[M_{Ad}\left(1-\frac{1}{N_d}\right)-K_z V_{dz}\right], \tag{31}$$

$$V_{dx}=-\frac{\beta_d}{2}M_{Ad}K_x\frac{\mathrm{d}^2\phi}{\mathrm{d}\xi^2} \tag{32}$$

and

$$V_{dz}=-\nu_m\frac{M_{Ad}}{K_z}\left(1-\frac{1}{N_d}\right). \tag{33}$$

By combining eqs (31)–(33) and taking $N_d = N_i = N$, the following expression is obtained:

$$K_x^2\frac{\beta_d}{2}\frac{\mathrm{d}^2\phi}{\mathrm{d}\xi^2}=-\left(1-\frac{1}{N}\right)(1+\nu_m). \tag{34}$$

From eqs (24) and (30), after some simplifications, we obtain

$$K_z^2\frac{\beta_d}{2}\frac{\mathrm{d}^2\psi}{\mathrm{d}\xi^2}=\nu_m M_{Ad}^2\frac{\mathrm{d}}{\mathrm{d}\xi}\left[\frac{1}{N}\frac{\mathrm{d}}{\mathrm{d}\xi}\left(1-\frac{1}{N}\right)\right]. \tag{35}$$

Using the moving coordinate (ξ) in eq. (25) and with the help of eq. (33), the following expression is obtained:

$$K_x^2K_z^2\frac{\beta_d}{2}\frac{\mathrm{d}^2(\phi-\psi)}{\mathrm{d}\xi^2}=-M_{Ad}^2(1+\nu_m)(N-1). \tag{36}$$

Using eqs (34)–(36) and after some algebraic manipulations, the following energy balance equation is obtained:

$$\frac{1}{2}\left(\frac{\mathrm{d}N}{\mathrm{d}\xi}\right)^2+U(N)=0, \tag{37}$$

where

$$U(N)=-\eta\left[M_{Ad}^2\left\{\left(1-\frac{1}{N}\right)+\frac{1}{2}\left(\frac{1}{N^2}-1\right)\right\}-K_z^2\left\{\frac{1}{2}\left(1-\frac{1}{N^2}\right)+\frac{1}{3}\left(\frac{1}{N^3}-1\right)\right\}\right] \tag{38}$$

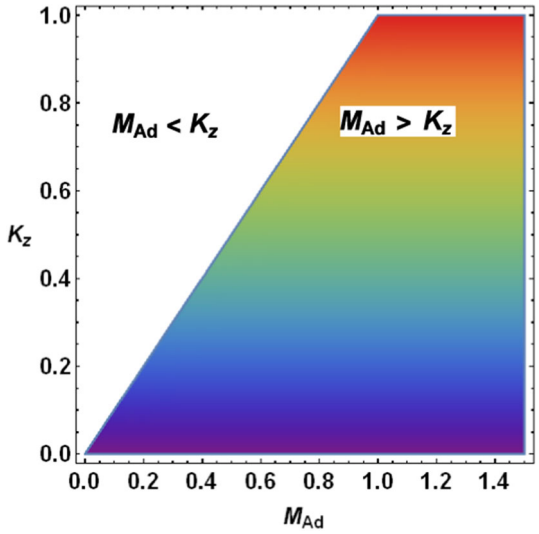

Figure 2. Region plot for $[\mathrm{d}^2U(N)/\mathrm{d}N^2]|_{N=1}$ when $\nu_m = 0.5 \times 10^{-4}$.

with

$$\eta=\frac{(1+\nu_m)N^6}{\nu_m(1-K_z^2)M_{Ad}^2}. \tag{39}$$

Equation (38) is called the Sagdeev pseudopotential. The Sagdeev pseudopotential $U(N)$ and $\mathrm{d}N/\mathrm{d}\xi$ are analogous to the potential energy and speed of a classical particle respectively.

5. Conditions of existence of DIAWs

The DIAWs can exist in the given plasma system, when the Sagdeev pseudopotential $U(N)$ satisfies the following conditions:

(i) $U(N) = (\mathrm{d}U(N)/\mathrm{d}N) = 0$ when $N = 1$.
(ii) $U(N_m) = 0$, where $N_m \neq 0$ represents the maximum amplitude of the waves.
(iii) $U(N) < 0$ between the points $N = 1$ and $N = N_m$.
(iv) $[\mathrm{d}^2U(N)/\mathrm{d}N^2]\big|_{N=1} < 0$.

From condition (iv), the range of the Mach number for the existence of DIA solitary waves can be obtained. Thus, for $N = 1$,

$$\frac{\mathrm{d}^2U(N)}{\mathrm{d}N^2}=-\frac{(1+\nu_m)}{\nu_m(1-K_z^2)M_{Ad}^2}(M_{Ad}^2-K_z^2)<0 \tag{40}$$

at

$$M_{Ad}^2 > K_z^2. \tag{41}$$

This suggests that the DIAWs travel at a speed larger than the cosine of the angle of propagation of the wave

with respect to the magnetic field. Now, in order to understand the behaviour of the Sagdeev pseudopotential $U(N)$ near $N = N_m$, $U(N)$ can be expanded by Taylor's series near $N = N_m$:

$$U(N \approx N_m) = -\frac{(1+\nu_m)}{\nu_m(1-K_z^2)M_{Ad}^2}(N_m-1)(N-N_m)N_m^2 \times(N_m M_{Ad}^2 - K_z^2), \quad (42)$$

and $U(N \approx N_m) < 0$ when $N_m < K_z^2/M_{Ad}^2$. As $K_z^2/M_{Ad}^2 < 1$, it is found that $N_m < K_z^2/M_{Ad}^2 < 1$. Thus, DIAWs with only density rarefactions can be formed. Figure 2 illustrates condition (iv) for the existence of DIAWs. The DIAWs exist in the shaded region, where

$$\frac{\mathrm{d}^2U(N)}{\mathrm{d}N^2} < 0$$

when $N = 1$. By carefully analysing this plot, it can be observed that the DIAWs exist only for $M_{Ad} > K_z$ (shaded region).

6. Parametric analysis

We have analytically shown that only density rarefactions can be associated with DIAWs which travel either at sub-Alfvénic or super-Alfvénic speed. In a typical magnetised laboratory dusty plasma with $B_0 = 3 \times 10^4$ G, $Z_i = 1$, $Z_d = 10^4$, $n_{i0} = 10^8$ cm^{-3}, $n_{d0} = 10^6$ cm^{-3} and $k_B T_i = 2$ eV [33], the existence condition of DIAWs, $\beta_d \ll m_i/m_d \ll 1$ has been achieved. Numerical analysis has been carried out by using the parameters of typical magnetised laboratory dusty plasma. In this section, we have discussed numerically the influence of different physical parameters on the characteristics of DIAWs.

The Mach number is conveniently used as a standard parameter to describe the effect of speed of a nonlinear structure on its characteristics, such as the amplitude and width of the solitary waves. In this investigation, we have defined the Mach number as a relative parameter which relates the speed of a nonlinear structure (V) to the dust Alfvén velocity (V_{Ad}), i.e., $M_{Ad} = V/V_{Ad}$. The Mach number $M_{Ad} = 1$ represents a parallel propagating non-dispersive wave travelling at the dust Alfvén speed V_{Ad}. So, we ignore this value of M_{Ad}. However, M_{Ad} can have these physically meaningful values: $0 < M_{Ad} < 1$ and $1 < M_{Ad}$. In figures 3 and 4, the effect of increase in the Mach number M_{Ad} on the characteristics of sub-Alfvénic and super-Alfvénic DIAWs has been shown respectively. It is observed that the increase in Mach number M_{Ad} for sub-Alfvénic DIAWs leads to a significant increase in both the amplitude and width. However, the increase in the Mach number M_{Ad} for super-Alfvénic DIAWs leads to the increase in amplitude but with a little effect on its width.

The effects of angle of propagation of the wave with respect to the magnetic field on Sagdeev pseudopotential and the corresponding soliton profile are shown in figures 5 and 6 respectively. The angle of propagation can be characterised by the direction cosine $K_z = \cos\theta$. Thus, $K_z = 0$ represents $\theta = 90°$ and $K_z = 1$ represents $\theta = 0°$. However, $K_z = 1$ (or $\theta = 0°$) corresponds to a purely non-dispersive parallel propagating dust Alfvén mode and $K_z = 0$ (or $\theta = 90°$) corresponds to transverse propagating dust magnetosonic waves. The DIAW propagates obliquely to the magnetic field and its dispersion occurs when the perpendicular wavelength $\lambda_\perp \approx \lambda_{\mathrm{eff}}$. Thus, we take only $0 < K_z < 1$ in numerical analysis. It is observed that the increase in K_z or the decrease in angle of propagation leads to the decrease in amplitude as well as width of both the sub-Alfvénic (see figure 5) and super-Alfvénic (see figure 6) DIAWs.

Figure 7 shows the hodographs which depict a relationship between the pseudovelocity $\mathrm{d}N/\mathrm{d}\xi$ and the pseudoposition N of a particle. The black curve corresponds to the sub-Alfvénic DIAWs represented by the black curve of figure 3 for (M_{Ad}, K_z)=(0.20,0.9) and the blue curve corresponds to the super-Alfvénic DIAWs represented by the black curve of figure 4 for (M_{Ad}, K_z)=(0.100012,0.9). Initially, the particle is stationary at $N = 1$ and under the effect of various forces in the plasma, its equilibrium is disturbed. The particle velocity increases along the axis $N < 1$, reaches a maximum and then reduces to zero at N_m while traversing an anticlockwise path. Again, the particle velocity increases and reaches maximum and then reduces to zero at $N = 1$. One closed orbit between $N = 1$ and $N = N_m$ represents the wavelength of a solitary wave. Pseudopotential force reflects the particle back when the particle velocity approaches zero [34]. Physically speaking, initially there is no perturbation in the particle number density, and perturbed n and equilibrium n_0 number densities are equal, i.e., $n = n_0$ (or $N = 1$). Perturbation starts increasing from $\xi = -\infty$ (although $n < n_0$), reaches the maximum value of $n = n_m$ ($N = N_m$) at $\xi = 0$ and again decreases such that perturbed and equilibrium number densities become equal, i.e., $n = n_0$ (or $N = 1$) at $\xi = \infty$.

7. Conclusions

The investigation of dust inertial Alfvén waves in an electron-depleted dusty plasma has been presented. Dispersion relation of DIAWs is modified by effective

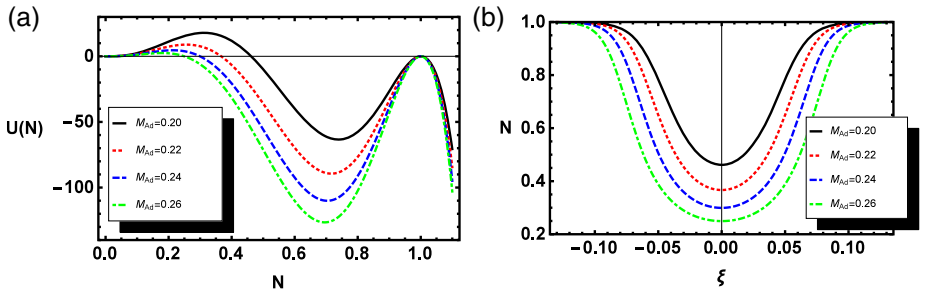

Figure 3. Effect of variation in the Mach number (via M_{Ad}) on sub-Alfvénic DIAWs at fixed values of $\nu_m = 0.5 \times 10^{-4}$ and $K_z = 0.9$.

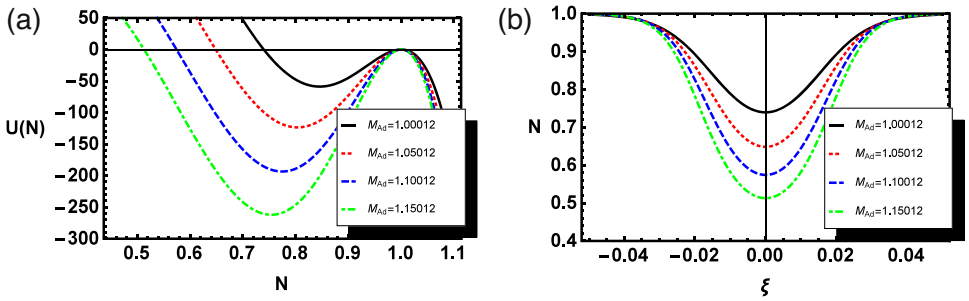

Figure 4. Effect of variation in the Mach number (via M_{Ad}) on super-Alfvénic DIAWs at fixed values of $\nu_m = 0.5 \times 10^{-4}$ and $K_z = 0.9$.

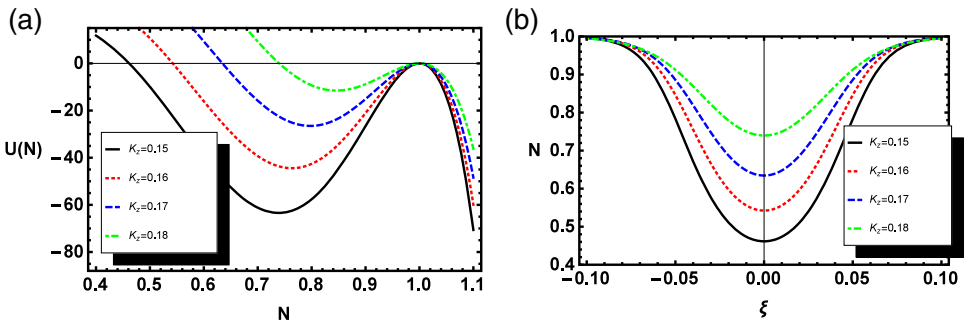

Figure 5. Effect of variation in angle of propagation (via K_z) on sub-Alfvénic DIAWs at fixed values of $\nu_m = 0.5 \times 10^{-4}$ and $M_{Ad} = 0.2$.

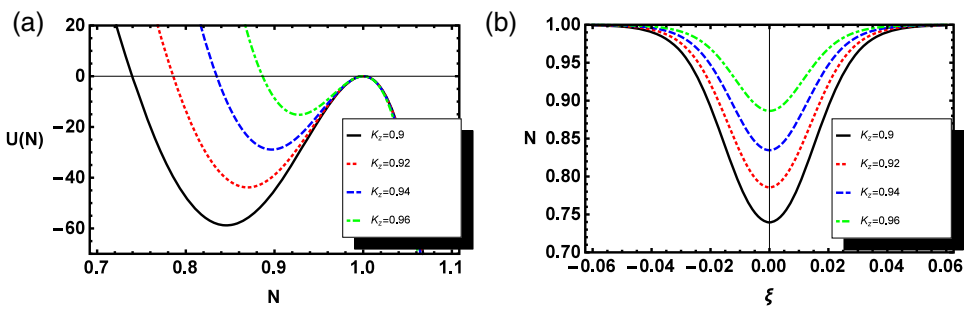

Figure 6. Effect of variation in angle of propagation (via K_z) on super-Alfvénic DIAWs at fixed values of $\nu_m = 0.5 \times 10^{-4}$ and $M_{Ad} = 1.00012$.

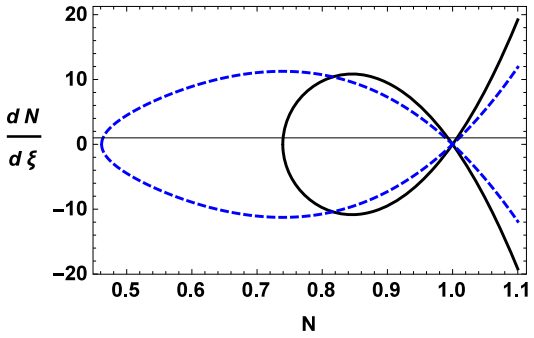

Figure 7. Hodographs corresponding to the Sagdeev pseudopotential given in eq. (38). Black curve corresponds to $(M_{Ad}, K_z) = (0.20, 0.9)$ and blue curve corresponds to $(M_{Ad}, K_z) = (0.100012, 0.9)$.

inertial length. By employing the Sagdeev pseudopotential method, an energy balance equation has been derived to study the nonlinear behaviour of DIAWs. From the expression of Sagdeev pseudopotential function, the parametric regime for the existence of DIAWs has been determined. It is observed that the DIAWs exist only for $M_{Ad} > K_z$. Only rarefactive DIAWs, travelling at sub- and super-Alfvénic speeds are observed in this plasma model. For sub-Alfvénic DIAWs, the increase in Mach number leads to the increase in amplitude as well as width of DIAWs. On the other hand, the increase in Mach number for super-Alfvénic DIAWs leads to the increase in only the amplitude, while having no influence on its width. The increase in angle of propagation for sub-Alfvénic DIAWs results in the decrease in amplitude while having no influence on its width. However, for super-Alfvénic DIAWs, the increase in angle of propagation leads to the decrease in both the amplitude as well as width of the DIAWs. This study may be useful in understanding the formation of nonlinear structures in laboratory plasma.

Acknowledgements

NSS gratefully acknowledges the support for this research work from Department of Science and Technology, Govt. of India, New Delhi under DST-SERB project No. CRG/2019/003988.

Appendix A. Linearisation and derivation of dispersion relation

The linearisation of eqs (10)–(17) is performed by assuming the following linearisation scheme: $n_i = n_{i0} + n_{i1}$, $n_d = n_{d0} + n_{d1}$, $v_{iz} = v_{iz1}$, $v_{dx} = v_{dx1}$, $v_{dz} = v_{dz1}$, $\phi_\perp = \phi_{\perp 1}$ and $\psi_\parallel = \psi_{\parallel 1}$. In this linearisation scheme, the quantities with the index '0' represent the unperturbed value of that quantity, while the quantities with the index '1' represent its first-order fluctuation. Thus, after the linearisation of eqs (10)–(14) and assuming all the first-order fluctuations to be of the form $A = Ae^{i(k_\perp x + k_\parallel z - \omega t)}$, we obtain the following set of equations respectively:

$$\omega n_{i1} = k_\parallel n_{i0} v_{iz1}, \tag{A.1}$$

$$\omega v_{iz1} = \frac{Z_i e}{m_i} k_\parallel \psi_{\parallel 1}, \tag{A.2}$$

$$\omega n_{d1} = k_\perp n_{d0} v_{dx1} + k_\parallel n_{d0} v_{dz1}, \tag{A.3}$$

$$v_{dx1} = \frac{c}{B_0 \Omega_d} \omega k_\perp \phi_{\perp 1} \tag{A.4}$$

and

$$\omega v_{dz1} = -\frac{Z_d e}{m_d} k_\parallel \psi_{\parallel 1}. \tag{A.5}$$

Combining eqs (15) and (16), and linearising it, we obtain

$$k_\perp^2 k_\parallel^2 (\phi_{\perp 1} - \psi_{\parallel 1}) = \frac{4\pi e}{c^2} [Z_i \omega^2 n_{i1} - Z_d \omega k_\parallel n_{d0} v_{dz1}]. \tag{A.6}$$

The linearisation of eq. (17) yields

$$Z_d n_{d1} = Z_i n_{i1}. \tag{A.7}$$

From eqs (A.1) and (A.2), we get

$$n_{i1} = \frac{k_\parallel^2}{\omega^2} \frac{Z_i e n_{i0}}{m_i} \psi_{\parallel 1}. \tag{A.8}$$

Similarly, from eqs (A.3)–(A.5), we get

$$n_{d1} = \frac{n_{d0} c}{B_0 \Omega_d} k_\perp^2 \phi_{\perp 1} - \frac{k_\parallel^2}{\omega^2} \frac{Z_d e n_{d0}}{m_d} \phi_{\parallel 1}. \tag{A.9}$$

Now, using eqs (A.8) and (A.9) in eq. (A.7), we get

$$\phi_{\perp 1} = \frac{1}{\lambda_{\text{eff}}^2} \frac{V_{Ad}^2 k_\parallel^2}{k_\perp^2 \omega^2} \psi_{\parallel 1}. \tag{A.10}$$

Using eqs (A.5), (A.8) and (A.10) in eq. (A.6), we get the required dispersion relation of the dust inertial Alfvén waves

$$\omega = \frac{k_\parallel V_{Ad}}{\sqrt{1 + k_\perp^2 \lambda_{\text{eff}}^2}}. \tag{A.11}$$

References

[1] H Alfvén, *Nature* **150**, 405 (1942)
[2] W H Bostick and M A Levine, *Phys. Rev. Lett.* **87**, 671 (1952)

[3] N F Cramer, *The physics of Alfvén waves* (Wiley-VCH Press, 2005)
[4] C K Goertz and R W Boswell, *J. Geophys. Res.* **84**, 7239 (2014)
[5] D J Wu and J K Chao, *J. Geophys. Res.* **109**, A06211 (2004)
[6] C K Goertz, *Rev. Geophys.* **27**, 271 (1989)
[7] M Horanyi and D A Mendis, *Astrophys. J.* **307**, 800 (1989)
[8] A A Samarian, B W James, S V Vladimirov and N F Cramer, *Phys. Rev. E* **64**, 025402 (2001)
[9] N C Adhikary, H Bailung, A R Pal, J Chutia and Y Nakamura, *Phys. Plasmas* **14**, 103705 (2007)
[10] M M Hossen, M S Alam, S Sultana and A A Mamun, *Eur. Phys. J. D* **70**, 252 (2016)
[11] K Singh, P Sethi and N Saini, *Phys. Plasmas* **25**, 033705 (2018)
[12] K Singh, Y Ghai, N Kaur and N S Saini, *Eur. Phys. J. D* **72**, 160 (2018)
[13] Y Ghai, N Kaur, K Singh and N S Saini, *Plasma Sci. Technol.* **20**, 74005 (2018)
[14] K Singh and N S Saini, *Phys. Plasmas* **26**, 113702 (2019)
[15] R K Shikha, N A Chowdhury, A Mannan and A A Mamun, *Eur. Phys. J. D* **73**, 177 (2019)
[16] K Singh and N S Saini, *Front. Phys.* **8**, 602229 (2020)
[17] R K Shikha, N A Chowdhury, A Mannan and A A Mamun, *Contributions to plasma physics*, https://doi.org/10.1002/ctpp.202000117 (2020)
[18] J Akter, N A Chowdhury, A Mannan and A A Mamun, *Indian J. Phys.*, https://doi.org/10.1007/s12648-020-01927-9 (2021)
[19] S Mahmood, H Ur-Rehman, M Z Ali and A Basit, *Contrib. Plasma Phys.*, https://doi.org/10.1002/ctpp.202000211 (2021)
[20] P K Shukla and A A Mamun, *Introduction to dusty plasma physics* (Institute of Physics, Bristol, 2002), pp. 3-4.
[21] C Yinhua, L Wei and M Y Yu, *Phys. Rev. E* **61(1)**, 809 (2000)
[22] A M Mirza, M A Mahmood and G Murtaza, *New. J. Phys.* **5**, 116 (2003)
[23] S Mahmood and H Saleem, *Phys. Lett. A* **338**, 345 (2005)
[24] N S Saini, B Kaur, M Singh and A S Bains, *Phys. Plasmas* **24**, 073701 (2017)
[25] M Salimullah and M Rosenberg, *Phys. Lett. A* **254**, 347 (1999)
[26] M A Mahmood, A M Mirza, P H Sakanaka and G Murtaza, *Phys. Plasmas* **9**, 3794 (2002)
[27] M Singh, N Kaur and N S Saini, *Phys. Plasmas* **25**, 023705 (2018)
[28] B B Kadomtsev, *Plasma turbulence* (Academic Press, New York, 1965) p. 82.
[29] P K Shukla, H Ur-Rahman and R P Sharma, *J. Plasma Phys.* **28**, 125 (1982)
[30] M K Kalita and B C Kalita, *J. Plasma Phys.* **35**, 267 (1986)
[31] N Kaur and N S Saini, *Astrophys. Space Sci.* **361**, 331 (2016)
[32] A Hasegawa and C Uberoi, *The Alfven wave* (Technical Information Center, U.S. Department of Energy, Washington, 1982)
[33] E Thomas, Jr, R L Merlino and M Rosenberg, *Plasma Phys. Controlled Fusion* **54**, 124034 (2012)
[34] E F El-Shamy, *Phys. Rev. E* **91**, 033105 (2015)